Forest Ecology and Management 569 (2024) 122156

Contents lists available at ScienceDirect

Forest Ecology and Management

journal homepage: www.elsevier.com/locate/foreco

Nationwide remote sensing framework for forest resource assessment in war-affected Ukraine

Viktor Myroniuk [a,*], Axel Weinreich [b], Vincent von Dosky [b], Viktor Melnychenko [c], Andrii Shamrai [c], Maksym Matsala [d], Matthew J. Gregory [e], David M. Bell [f], Raymond Davis [g]

[a] *National University of Life and Environmental Sciences of Ukraine, Ukraine*
[b] *Unique land use GmbH, Germany*
[c] *Ukrainian Forest Management Planning Association, Ukraine*
[d] *Swedish University of Agricultural Sciences, Sweden*
[e] *Oregon State University, Department of Forest Ecosystems and Society, USA*
[f] *USDA Forest Service, Pacific Northwest Research Station, USA*
[g] *USDA Forest Service, Pacific Northwest Region, USA*

ARTICLE INFO

Keywords:
NFI
Forest cover
Tree species
Forest attributes
Model-assisted estimation
Sentinel 2

ABSTRACT

The full-scale Russian invasion of Ukraine in 2022 has had a dramatic impact on Ukrainian forestry and forest resources. In this situation, the ability of the National Forest Inventory (NFI) to update forest information at the state level is very limited due to the large territory which is inaccessible for field data collection. This study presents an approach for the combined use of different sources of field observations and remotely-sensed forest vegetation imagery to produce a time series (TS) to characterize forest conditions and changes across Ukraine. First, we created a forest cover map for 2023 using reference information obtained through visual interpretation of high-resolution imagery at NFI plot locations. Then, we used newly collected NFI data (2021–2023) in areas controlled by the government of Ukraine territories, and retrospective Forest Management Planning (FMP) data (2019–2020) as a reference to map dominant tree species and forest attributes. Finally, we used a model-assisted estimation procedure to obtain information on forest resources over Ukraine, including Russian-occupied territories. We used a random forest classifier to map forest cover and dominant tree species, and gradient nearest neighbor (GNN) imputation to predict continuous forest attributes. Accuracy of the forest map over ecoregions correlates with forest cover; thus, we obtained the highest accuracy (90–98 %) for ecozones with forest cover of more than 40 %, and the lowest (about 60–72 %) for ecozones with forest cover of 2–7 %. The overall accuracy of dominant species classification was 76.3±1.5 %, the accuracy of mapping pure coniferous forest was 87–92 %, while it ranged from 35 % to 85 % for mixed deciduous forest. We found that FMP data greatly contributed to mapping forest attributes in inaccessible areas. The GNN model performed better in predicting basal area and growing volume ($R^2 = 0.44$–0.47), but we found that predicting mean age, diameter, and height with optical data was still challenging ($R^2 = 0.10$–0.35). The study revealed that the total forest area in Ukraine is 11.2±0.2 million ha and the mean growing stock volume is 251±5 $m^3 \cdot ha^{-1}$. Of that amount, about 1.7 million ha could be potentially affected by the war (temporarily occupied, contaminated, damaged, etc.), storing about 377 ± 15 million m^3 of growing volume. Within this area, we identified about 67 thousand ha with some degree of canopy disturbance. This study creates a framework for further monitoring of forest resources in Ukraine and provides effective tools for spatial assessment of war-induced forest damage.

1. Introduction

The full-scale Russian invasion in 2022 caused extensive forest damage in Ukraine (Irland et al., 2023; Matsala et al., 2024; Shumilo et al., 2023), while ground-based assessment of the impact has been constrained by many factors. In particular, about 30 % of the country's territory were not controlled by the Ukrainian government. It was also impossible to collect field data in many places close to the front lines or

* Correspondence to: 15 Heroiv Oborony St., Kyiv 03041, Ukraine.
E-mail address: victor.myroniuk@nubip.edu.ua (V. Myroniuk).

https://doi.org/10.1016/j.foreco.2024.122156
Received 20 May 2024; Received in revised form 10 July 2024; Accepted 13 July 2024
Available online 24 July 2024

in areas contaminated by unexploded ordnance and land mines. Therefore, Ukraine's post-war recovery requires an effective framework harnessing remote sensing and field observation data to address information needs on forest change and forest cover losses due to war-induced damage.

Accurate information collected through National Forest Inventories (NFI) using field and remote sensing (RS) observations provides important support to forest policy and forest management. In recent decades, RS data have been increasingly used in forest inventory and monitoring programs in many regions of the world (Breidenbach et al., 2020; Coops et al., 2023; Davis et al., 2022; Lister et al., 2020). Benefiting from the ability to cover large geographical areas in a brief time, RS technologies can sufficiently improve NFI procedures (i.e., post-stratification, model-assisted estimation, etc.) by 1) imputation of NFI plot data to the larger area outside of sample plots, 2) producing time series (TS) maps to track changes in between plot remeasurement cycles and for areas that may be inaccessible for field data collection (Fassnacht et al., 2024; McRoberts et al., 2014). Thus, satellite-based RS technologies expand the role of NFI from statistical estimates of mean or total values of forest attributes at the national scale to spatially explicit characterization of forest structure at different spatial domains (McRoberts and Tomppo, 2007).

Free open access to multispectral imagery from the NASA Landsat and the ESA Copernicus Sentinel programs, coupled with the increased capacity of modern cloud-based computing platforms (e.g., Gorelick et al., 2017), has contributed to the development of efficient land cover and forest monitoring approaches in a global context (Hermosilla et al., 2022; Hislop et al., 2021; Senf and Seidl, 2021). In terms of forest inventory, the processing of satellite imagery in conjunction with NFI data has led to significant advances in the mapping and assessment of forest structure attributes (Lister et al., 2020). A variety of RS-based approaches have been used to map tree species (Welle et al., 2022), forest growing stock volume (GSV) and live biomass (LB) (Chirici et al., 2020; Kennedy et al., 2018), age (Maltman et al., 2023), height (Matasci et al., 2018), and other important characteristics of forest stands that have been thoroughly summarized in review papers (Brosofske et al., 2014; Fassnacht et al., 2016). The RS-derived maps provide auxiliary information suitable for estimation of forest attributes within small areas of interest (Bell et al., 2022; McRoberts, 2012).

The ability to monitor forest conditions using remote sensing technologies has been greatly improved by advances in satellite TS processing. Various algorithms developed in recent years have been proposed to detect abrupt and gradual changes in forest cover as well as to produce stable synthetic series of clear observations (Zhu, 2017). The synthetic images can be used instead of original data in classification and imputation providing temporally consistent results based on spectral trajectories observed for individual pixels (Chen, 2021; Ohmann et al., 2012). The choice of temporal segmentation algorithm depends on the complexity of change processes, information needs, and computing capabilities. Some algorithms, such as LandTrendr (Kennedy et al., 2010), detect change and fit reflectance trajectories at annual time steps. Others leverage within-year variation in satellite imagery, such as the Continuous Change Detection and Classification (CCDC) algorithm (Zhu and Woodcock, 2014), processes all available cloud-free observations and can characterize seasonal variability of spectral observations within temporal segments. Therefore, CCDC may be better suited for mapping and monitoring applications with temporally dense, high-quality satellite observations over a long time period (Pasquarella et al., 2022). Time-series of synthetic imagery, such as CCDC-fitted TS, are advantageous in monitoring programs in terms of improved coherence of predictions made for the same location over time (Gorelick et al., 2023; Xian et al., 2022), or for studies dealing with retrospective field data collected in the past (Myroniuk et al., 2022). Although CCDC can be used with various multitemporal datasets, its application with satellite imagery other than Landsat TS, such as Sentinel data, is still limited (Bullock et al., 2022). It is likely that interest in Sentinel TS will continue to grow as it covers a wider time range.

Machine learning algorithms have become common tools for classifying discrete forest conditions (e.g., forest type, species) and predicting continuous forest characteristics (e.g., biomass, age, height). The random forest (RF) classifier has been used more frequently than other nonparametric approaches due to its ability to work with both discrete and continuous forest variables (Chirici et al., 2020; Riley et al., 2016). Characterizing many related forest attributes using independent models can potentially lead to unrealistic combinations of predicted values. Therefore, the use of multivariate modeling, such as nearest neighbor imputation, has attracted substantial interest in vegetation mapping (Henderson et al., 2014, 2019). A multivariate property of nearest neighbor techniques has made them particularly attractive for operational use with RS and forest inventory data (Chirici et al., 2016). Recent studies have shown good potential for implementing nearest neighbor imputation in combination with temporal segmentation algorithms (Myroniuk et al., 2022; Ohmann et al., 2012) for spatially explicit characterization of forest attributes. Wall-to-wall products representing mapped forest attributes at fine spatial scales provide a statistical framework for model-assisted or post-stratified estimation procedures in NFI (McConville et al., 2020).

Accurate maps of dominant tree species are an essential output of forest inventories, providing a baseline for reporting on a wide range of forest attributes (Breidenbach et al., 2021). The large number of publications reflects the continued interest in this topic, highlighted in the review paper by Fassnacht et al. (2016). Methodologies for tree species mapping have improved significantly over the last decade using different types of satellite data and phenology-based classification. For example, Hemmerling et al. (2021) showed that capturing the phenology of species during the leaf-on period in Germany can help to increase accuracy of classification results. Other environmental variables (soil, climate, topography) could only slightly improve the classification accuracy of minor tree species. In most cases, coniferous and deciduous species groups can be classified with the highest accuracy, while classification of individual species in mixed stands remains challenging (Blickensdörfer et al., 2024).

Forest characterization using RS technologies and NFI data in Ukraine is a high priority. First, it is important to support forest management with regularly updated statistics and maps in line with existing practices in other European countries. Second, the RS-supported assessment of forest resources at national level is the only feasible approach given the scale and long-term effects of the Russian invasion of Ukraine (e.g., inaccessible plots). Third, regular monitoring of forests in temporarily occupied and war-affected areas is essential to provide timely insights into forest damage. Additionally, officially recognized assessments of forest cover loss due to war damage require accurate information on pre-war forest conditions. To make such an assessment, researchers mostly rely on their own spatial data sets created for the specific target (Matsala et al., 2024; Shumilo et al., 2023) which can lead to discrepancies in estimates. Given the importance of the topic, we present a nationwide framework for mapping and assessing forest characteristics in Ukraine using Sentinel 2 TS and officially recognized forest inventory data, such as NFI and retrospective stand-wise forest inventory (Forest Management Planning (FMP)) data. This study aims not only overcome limitations to traditional NFI caused by war-related plot inaccessibility, but also contribute to reliable assessments of war-induced forest damage since the beginning of the invasion in 2022.

2. Materials and methods

2.1. Study area

With an area of 603,628 km^2, Ukraine is the largest country that is entirely within Europe. In 2014, Ukraine lost control of about 43,000 km^2 of the Crimean Peninsula annexed by Russia and takeover territory in the Luhansk and Donetsk regions (oblasts). After the full-scale invasion in 2022, Russia occupied additional Ukrainian territory, bringing the total to almost 30 % of the country's territory affected by the war (Fig. 1).

According to the latest state forest resource assessment, 15.9 % of Ukraine is covered by forest (Handbook, 2012). The percentage of forested area varies from 5 % to 12 % in the eastern and southern oblasts, from 15 % to 35 % in the central and northern oblasts, and from 30 % to 50 % in the western mountainous oblasts of Ukraine. However, actual forest cover may be higher due to unaccounted natural forest regrowth on former farmlands abandoned after the collapse of the Soviet Union and a series of land reforms in the 2000s (Matsala et al., 2021; Myroniuk et al., 2022; Stefanski et al., 2014).

Ukraine's forests consist of more than 30 tree species. The most common are Scots pine (*Pinus sylvestris* L.), European oak (*Quercus robur* L.), European beech (*Fagus sylvatica* L.), Norway spruce (*Picea abies* L.), silver fir (*Abies alba* L.), silver birch (*Betula pendula* Roth.), black alder (*Alnus glutinosa* (L.) Gaerth), European hornbeam (*Carpinus betulus* L.), and European ash (*Fraxinus excelsior* L.). Coniferous species dominate, due to the prevalence of monocultures of pine in the northernmost oblasts in Ukraine and spruce and fir stands in the Carpathian montane forests.

Ukraine is mainly a non-mountainous country. The Outer Eastern Carpathians have a maximum elevation of 2061 m, while the highest peaks of the Crimean Mountains reach 1545 m. The climate becomes more continental from the northwest to the southeast, with less rainfall, lower winter temperatures and hot summers. The distribution of forests and their characteristics are linked to gradients of environmental conditions. The structure of mountainous forests is mainly explained by altitudinal gradients (e.g., spruce dominates at elevations of more than 800 m. in the Carpathians). The relationships between the spatial patterns of forests, their dominant functions in different parts of Ukraine, and environmental factors were accurately captured by Gensiruk (1992) who proposed a classification of Ukraine using six main ecozones (Fig. 1).

2.2. Reference data

2.2.1. NFI sample plots

Sample plots of the first NFI cycle were collected during 2021–2023 in 18 of the 25 oblasts of Ukraine. Field work was caried out before the Russian invasion or in areas not affected by the military operations since 2022. The nationwide NFI sample design uses a random allocation of clusters of plots within a systematic reference grid of 5 × 5 km (Myroniuk et al., 2022; Storozhuk and Polley, 2017). Each cluster contains fixed-area sample plots spaced 420 m apart along the sides of a square. The Ukrainian NFI utilizes nested plots that consist of four

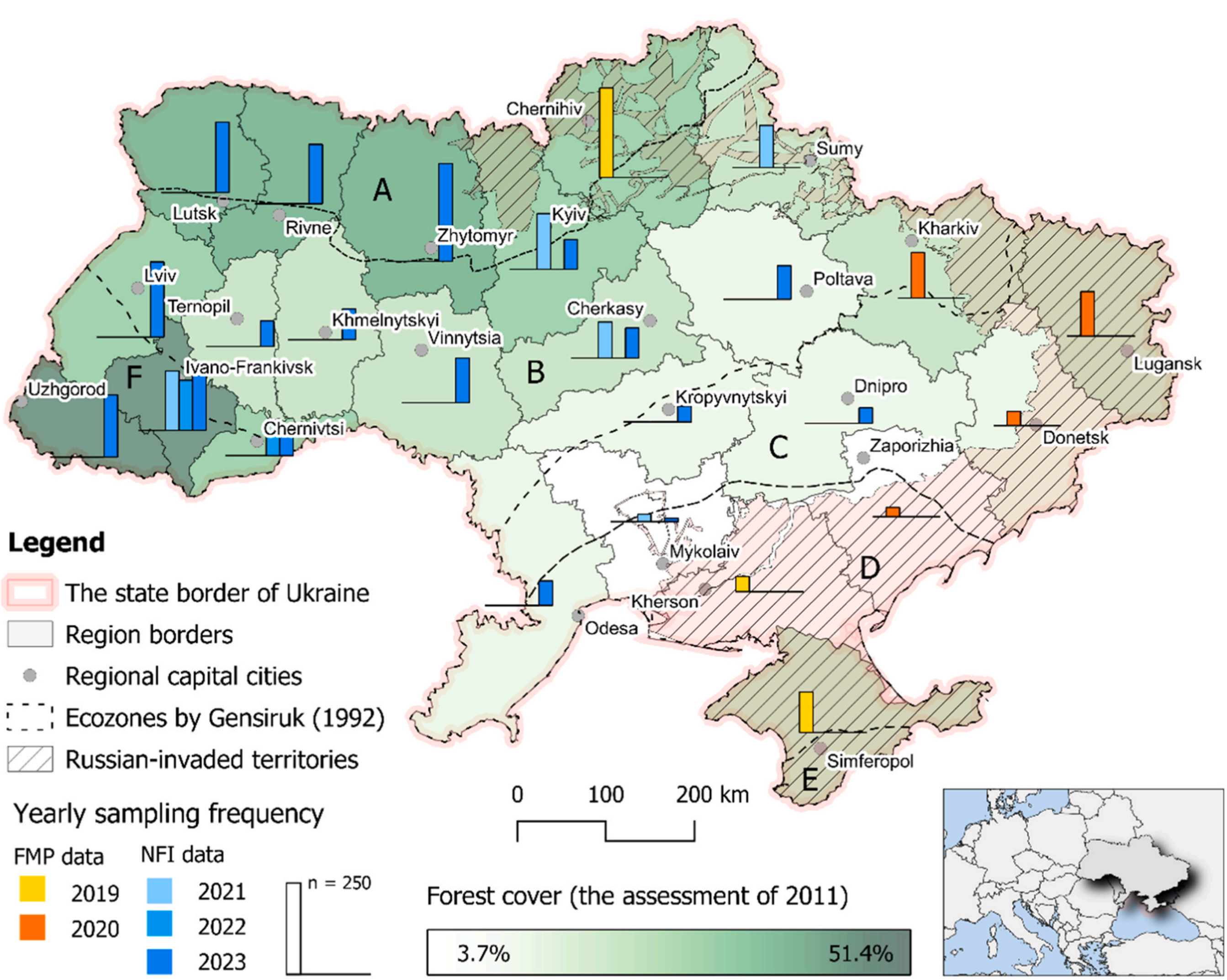

Fig. 1. Location of the study area and field sample size. A-F represent ecozones of Ukraine according to Gensiruk (1992): A – Polissia; B – Forest steppe; C – Northern steppe; D – Southern steppe; E – Crimean Mountains; F – Carpathians. Oblast boundaries (color-coded by 2011 estimated forest cover (Handbook, 2012)) and maximum extent of Russian invasion (2022–2023) are provided. Bar plots represent number of NFI plots collected in 2021–2023.

concentric subplots (500 m^2, 250 m^2, 50 m^2, and 10 m^2). Trees on each subplot are measured based on the corresponding minimum diameters (26 cm, 14 cm, 6 cm, and 2 cm, respectively). During the referenced period, approximately 4100 plots were sampled in the field across Ukraine, of which 2634 were used in this study. We selected only sample plots that did not straddle different stands and were at least 75 % forested. Per hectare estimates of forest attributes were calculated using measurements of sampled trees corresponding to the subplot area expansion factors (Kershaw et al., 2016). We used proportional distribution of species basal area (BA) to identify dominant species on each sample plot. For dominant species, we obtained quadratic mean diameter at breast height (DBH), mean stand height (HT), and mean age. The volume of growing stock was estimated using tree stem volume equations developed for major species in Ukraine (Bilous et al., 2020).

2.2.2. FMP reference polygons

FMP data were used for seven oblasts where the NFI field work was not possible (Fig. 1). The FMP had formerly been the only source of information on forests in Ukraine, collected periodically (every ten years) through a stand-wise forest survey. The data structure of the FMP is similar to that of the NFI, but it mainly represents average forest attributes observed within forest stands (1 ha – 15 ha) with many of them being estimated by experts rather than measured in the field. We used the most recent FMP data from 2019 and 2020 in this study. For the Crimea, which was annexed in 2014, forest stand attributes were updated to 2019 using past FMP data (2012) and growth models (Bilous et al., 2020).

We attempted to extract a balanced sample that approximated the one-phase (2023) sampling intensity of the NFI reference grid. Therefore, we sampled forest stands using NFI plot locations. Given the non-uniform spatial structure of the stands, trained interpreters visually analyzed high resolution Google Earth imagery in conjunction with the FMP information (i.e., species, age, density, etc.) to outline training polygons at "typical locations" within the stands. Training polygons were rectangular in shape with an area of 0.1–0.8 ha. Both NFI and FMP data were used to map forest structure attributes across Ukraine.

2.2.3. Visually interpreted data

Visually interpreted data were used for land cover classification and forest mask extraction. A team of interpreters analyzed 19,370 plot locations corresponding to the one-year phase (2023) of the Ukrainian NFI. Visual interpretation was performed using the Collect Earth plugin (Bey et al., 2016) and a two-level classification scheme. This scheme included seven main land cover classes (forest, other woody vegetation, grassland, cropland, wetland, water, urban and other unproductive land), which in turn had several subclasses. Each photo-interpreted plot was assigned the year in which the plot showed no land cover change within at least a one-year window, as well as the confidence in the interpretation. The interpretation was carried out for 2019–2023 that corresponded to the period for which we obtained a high-quality Sentinel 2 TS.

2.3. Temporal segmentation of Sentinel 2 TS

We used surface reflectance Sentinel 2 Level 2 A TS acquired from March 2017 to November 2023. Images were screened for clouds and cloud shadows using the Scene Classification band. The following spectral data were used in the analysis: the original spectral bands, the first three primary components (brightness, greenness, and wetness) of the Tasseled-Cap Transformation (Crist & Cicone, 1984) and the Normalized Burn Ratio (NBR) (Key & Ben-son, 2006). All selected bands and indices were resampled to 20-m spatial resolution.

The Sentinel 2 TS were temporally smoothed using the Google Earth Engine implementation of the CCDC algorithm (Gorelick et al., 2023; Zhu and Woodcock, 2014). This approach is based on a harmonic regression, that captures cyclic patterns of spectral reflectance according to vegetation phenology throughout the year. The CCDC algorithm uses TS of spectral data at pixel level and split them into successive segments corresponding to periods with no land cover change. The harmonic model coefficients can be used both to create annual and seasonal synthetic images used as predictor variables in classification and mapping (see Section 2.4 for additional details). Given the computationally extensive nature of the CCDC algorithm, the image processing was performed using a regular 0.5 × 1-degree grid seamlessly covering the territory of Ukraine, then fitted images were stored as Google Earth Engine assets.

The reference plots were intersected with the corresponding time segments of the Sentinel 2 TS. We also added information on location (longitude and latitude) and elevation to our datasets. Thus, we obtained a training data set used to classify forest cover and dominant species, and to predict forest attributes.

2.4. Mapping workflow

2.4.1. Mapping forest cover and dominant tree species

We used two random forest (RF) models (Breiman, 2001) to map forest cover and dominant species (Table 1). The models were trained using 1) synthetic values of Tasseled-Cap Transformation components and NBR for the beginning (April 15), middle (June 15), and end (October 15) of the leaf-on period, 2) harmonic model coefficients and derivatives (phase, amplitude), and 3) coordinates and elevation. The RF models were developed with default hyperparameters, i.e., the number of decision trees in the ensemble was 500 and the number of variables per split was the square root of the number of predictor variables. First, a classifier was created to map forest and other land cover categories using visually interpreted data. Then, a new classifier was trained using NFI and FMP data to map dominant species within the forest mask classified with the first RF model.

Dominant species were identified by the highest BA proportion for sample plots. Approximately 50 % of all plots represented "pure" (or monoculture) stands, i.e., where at least 80 % of the overstory's BA consisted of a single species (Bravo-Oviedo et al., 2014). The highest proportion of monocultures (60 %) was observed within the Polissia, while mixed-species forests were predominantly associated with the Crimean Mountains (only 25 % of sample plots represented "pure" stands). We separated the most important individual species, while others have been grouped according to their typical habitat and environmental niches: 1) pine; 2) spruce and fir; 3) oak; 4) beech; 5) deciduous species with high life expectancy (maple, ash, linden, etc.); 6) deciduous species with low life expectancy (birch, alder, poplar, willow); 7) hornbeam.

2.4.2. Predicting forest attributes

Forest attributes were mapped using the gradient nearest neighbor (GNN) imputation algorithm (Ohmann and Gregory, 2002) that was implemented in Google Earth Engine (Myroniuk et al., 2022). The GNN finds nearest neighbors in a reduced feature space of environmental

Table 1
Predictor variables used in the study.

Variable type	Name	RF classification		GNN imputation
		Forest cover	Tree species	
Spectral indices fitted for the 15th of April, June, October	Tasseled-Cap Transformation components	+	+	+
	NBR	+	+	–
CCDC harmonic model	Coefficients	+	+	–
	Phase, amplitude	+	+	–
Environmental data	Coordinates	–	+	+
	Elevation	–	+	+

The plus sign indicates that variable was used in the model variables (Table 1) using canonical correspondence analysis. This is a multivariate technique that simultaneously predicts a set of response variables. Therefore, we constructed the matrix of response variables using total BA and per hectare estimates of BA observed for individual species at sample plots. Following the approach of Bell et al. (2015), we identified the seven nearest neighbors for each pixel and calculated weighted values of BA, GSV, age, DBH, and HT for each 20-m Sentinel 2 pixel using weights empirically derived to approximate a large bootstrap sample.

2.4.3. Assessing map accuracies

The performance of the RF models (forest cover and dominant species) was assessed using k-fold cross-validation (James et al., 2013). The resulting lists of observed and predicted values were used to construct confusion matrices using the "good practices" protocol (Olofsson et al., 2014). The RF models were evaluated using 95 % confidence intervals of producer's accuracy, user's accuracy, and overall accuracy.

We assessed the accuracy of the GNN models using the first seven independent nearest neighbors, i.e., excluding self-imputed reference plots (*sensu* (Bell et al., 2021)). This is a modified leave-one-out procedure for assessing the accuracy of nearest neighbor models proposed by Ohmann and Gregory (2002). We calculated R^2 using actual and predicted observations for all continuous variables.

2.4.4. Estimation of forest area and forest attributes

In this study, we used the biophysical definition of forest as an area covered by woody vegetation with a predefined minimum canopy cover (>50 %) observed at 20 × 20 m pixels regardless of its legal status. Pixel areas obtained directly from maps were adjusted according to the "good practice" estimation procedure (Olofsson et al., 2014) that incorporates confusion between map classes.

Means and variances of continuous forest attributes were calculated using generalized regression (GREG) estimators, following McConville et al. (2020) guidelines.

GREG estimator for means:

$$\widehat{\mu}_y = \frac{1}{n}\sum_{i\epsilon S}(y_i - \widehat{m}(x_i)) + \frac{1}{N}\sum_{i\epsilon u}\widehat{m}(x_i), \tag{1}$$

GREG estimator for variances:

$$\widehat{V}\left(\widehat{\mu}_y\right) = \left(1 - \frac{n}{N}\right)\frac{1}{n}\frac{1}{n-1}\sum_{i\epsilon S}(y_i - \widehat{m}(x_i))^2, \tag{2}$$

confidence interval for estimated means:

$$\widehat{\mu}_y \pm t_{(n-1;1-\alpha/2)} \bullet \sqrt{\widehat{V}\left(\widehat{\mu}_y\right)}, \tag{3}$$

where N is the finite number of the population u units (pixels); n is the number of selected units (plots) for the sample S; y_i is the observed value for i-th unit; $\widehat{m}(x_i)$ is the predicted value for the i-th unit given auxiliary data x; $t \approx 2$ for a 95 % confidence interval.

2.4.5. Quantifying war impact on forests

Forest losses were identified as a difference in NBR (dNBR) values extracted from Sentinel 2 TS for September 2021 versus September 2023. We used dNBR greater than 0.1 from the original work by Key and Benson (2006) to separate forest losses from stable forests. The 2021 forest mask was used to identify forest losses that occurred in 2022 and 2023 in forests.

3. Results

3.1. Map accuracy

3.1.1. Accuracy of forest map

The forest area of Ukraine was mapped with high user's (91.1 ± 1.0 %) and producer's (92.2 ± 1.0 %) accuracies, while overall accuracy of land cover classification was 88.1 ± 0.5 %. According to the obtained results, forests in Ukraine occupy an area of 11.2 ± 0.2 million ha. The RF classification model showed different performance across Ukraine, where forest maps achieved higher accuracy for ecozones that have the highest percentage of forest cover (Fig. 2). The results for Northern and Southern steppes with less than 8 % forest cover were the least accurate, and the confidence intervals for both user's and producer's accuracies were wider.

3.1.2. Accuracy of dominant species map

The overall accuracy of the dominant species map was 76.3±1.5 %. The highest user's and producer's (87–92 %) accuracies were obtained for Scots pine as well as for Norway spruce and silver fir forest stands (Fig. 3). Misclassifications between these coniferous species were minimal because they are mostly associated with different ecozones. For example, spruce and fir forests are typical for the Carpathian Mountains, where the share of pine forests is minimal. Similarly, we observed the highest accuracy for beech, which dominates other deciduous species in the Carpathians. For other deciduous species, user's and producer's accuracies ranged between 35 % and 85 %. However, the two groups of mixed deciduous species (i.e., ash, linden, maple, black locust and birch, alder, poplar) also showed accuracies higher than 60 %, supporting our decision to combine tree species according to their ecological niches (i.e., forest types). Unlike forest cover, we did not find any relationships between map accuracy and the proportion of the species in the total forest area of Ukraine.

3.1.3. Accuracy of the GNN models

GNN imputation showed variable efficiency in predicting BA. The R^2 values varied from low ($R^2 = 0.1$) for the Forest steppe, to significantly better ($R^2 = 0.3$) for the Polissia, to moderate ($R^2 = 0.5$) for the Carpathians. Since we did not have enough field observations for the Northern and Southern steppes to test the model efficiency, we combined these ecozones with the more forested Crimean Mountains and obtained $R^2 = 0.5$. We also found that observed and predicted values at a cluster level have smaller deviations than in the case of individual plot observations (Fig. 4).

We used the same GNN model to simultaneously map different forest attributes (Table 2). The predictive performance of the model was better for BA and GSV ($R^2 > 0.4$), while mapping other forest attributes using Sentinel 2 optical satellite data is still challenging. This is especially the case for such forest attributes as DBH ($R^2 = 0.10$) and stand age ($R^2 = 0.23$) that are not directly correlated with stand biomass.

3.2. Spatial assessment of stand attributes

We developed the map of seven dominant tree species groups, which allowed us to obtain estimates of forest attributes at the ecozone level as the lowest spatial domain. There are varying spatial patterns of tree species composition in Ukraine. In particular, Scots pine forests mainly dominate within the northernmost Polissia ecozone. Forests in the Carpathians are composed by Norway spruce, silver fir, and European beech stands. Mixed deciduous forests are common in the rest of the territory of Ukraine (Fig. 5).

We found that the mean growing stock volume in Ukrainian forests is 251 ± 5 $m^3 \cdot ha^{-1}$. However, GSV values vary significantly among the tree species and ecozones across Ukraine (Fig. 6). Spruce, fir, and beech forest stands that dominate in the Carpathians can exhibit mean GSV of 400 $m^3 \cdot ha^{-1}$. Oak and pine forests are generally characterized by mean GSV up to 300 $m^3 \cdot ha^{-1}$. The lowest mean values of GSV (below 300 $m^3 \cdot ha^{-1}$) are typical for the Steppe and Crimean Mountains ecozones regardless of species.

The results of the study indicate that grouping forest characteristics by dominant species groups narrows the 95 % confidence intervals for estimates of forest attributes. The standard errors of the estimated means

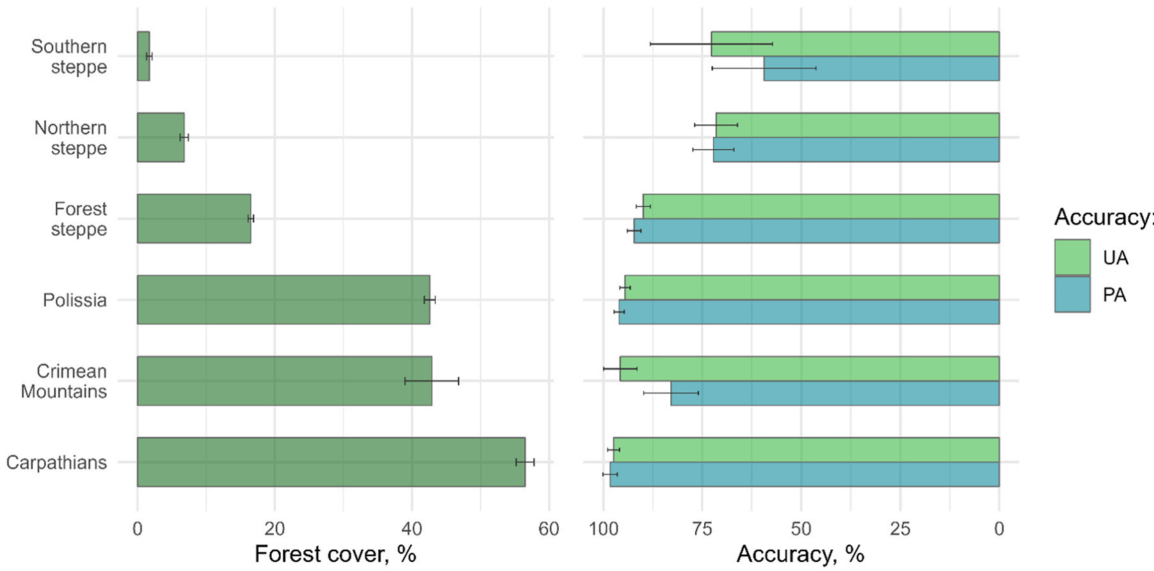

Fig. 2. Distribution of forest area in Ukraine by ecozones and associated map accuracies. Error bars indicate 95 % confidence intervals of estimated values. UA – user's accuracy, PA – producer's accuracy.

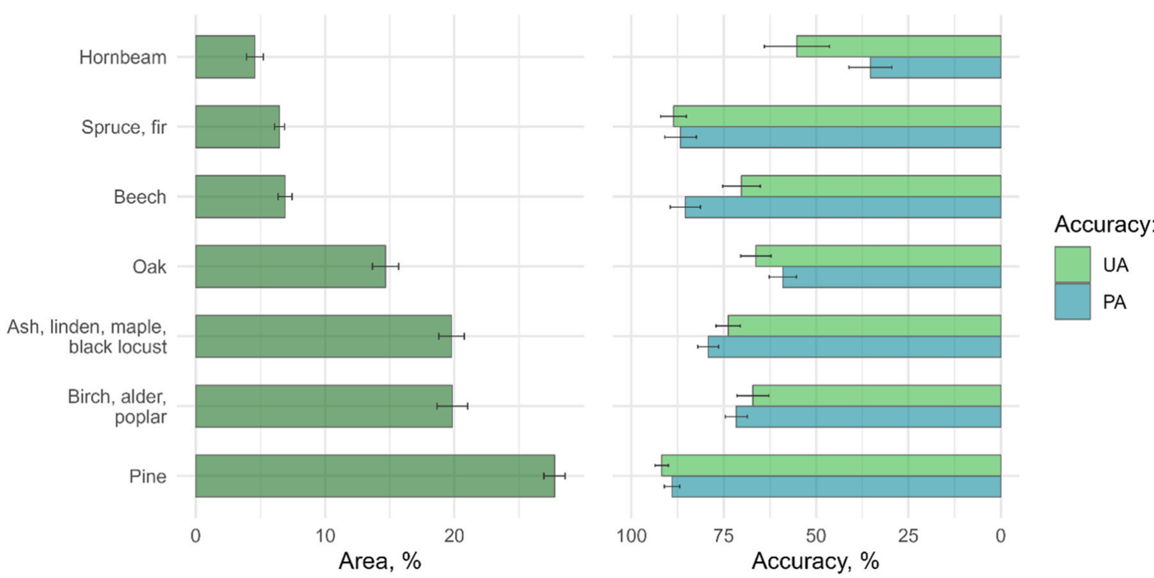

Fig. 3. Distribution of forest area by dominant species and associated map accuracy. Error bars indicate 95 % confidence intervals of estimates. UA – user's accuracy, PA – producer's accuracy.

varied between 1.0 % and 2.0 % for all species combined, between 1.5 % and 3.0 % for the groups of coniferous and deciduous species, and between 2.1 % and 8.6 % for individual species (Table 3). This is also the case when comparing the results at the national level (all species) with those obtained for the ecozones (Table 4). In particular, we calculated mean values of forest attributes for all species within ecozones with larger standard errors (1.9–4.0 %) than those obtained at the national level.

3.3. Quantifying war damage

The Russian invasion of Ukraine caused significant forest losses (Fig. 7). We identified at least three hotspots with the largest forest losses in the north (Chornobyl Exclusion Zone), east (Luhansk and Kharkiv oblasts), and south (Kherson oblast) of Ukraine. It is important to note that the loss of forest area was highest in the war-affected areas, although the areas most affected by the war are also the areas with the lowest forest cover.

We found about 1.7 million ha of forests, accounting for 15 % of the total forest area in Ukraine, could be potentially affected by the war, including damage caused by shelling, unexploded ordnance, management limitations due to proximity to the frontline or Russian border. These forests store about 377 ± 15 million m^3 of growing volume which is equivalent to 14 % of the growing volume at the national scale. The analysis of dNBR values revealed that 67 thousand ha experienced various levels of canopy disturbance (Fig. 8). About half of these areas (31 thousand ha) are characterized by a low level of disturbance, which may indicate partial loss of canopy cover.

4. Discussion

4.1. Addressing forest information needs in war-affected Ukraine

Remote sensing-based approaches have been widely integrated into

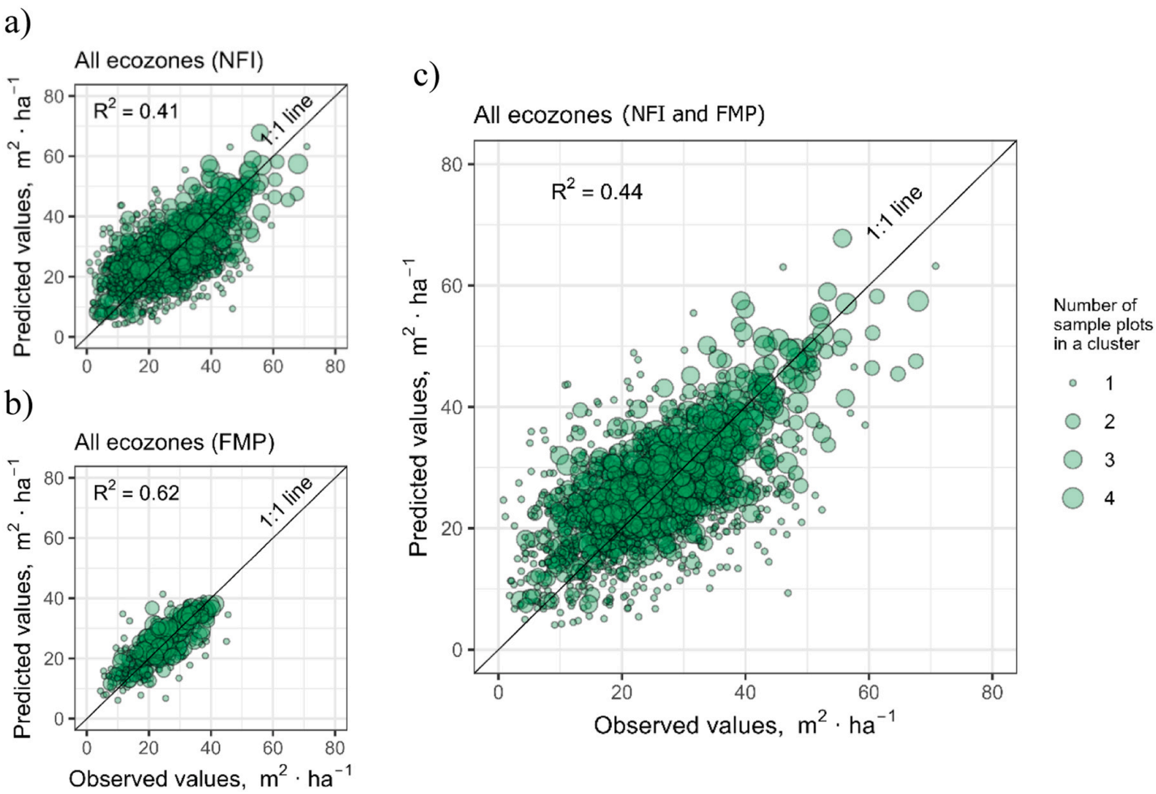

Fig. 4. Observed versus predicted BA for the GNN models developed using NFI only (a), FMP only (b), and NFI with FMP data (c) across Ukraine.

Table 2
Accuracy of the GNN imputation model (n = 3334) across Ukraine.

Forest attribute	Mean attribute value		Normalized RMSE	R^2
	Observed	Predicted		
BA, $m^2 \cdot ha^{-1}$	26.6	27.3	0.30	0.44
Age, years	60	62	0.33	0.23
DBH, cm	28.6	29.3	0.31	0.10
HT, m	21.4	22.0	0.25	0.35
GSV, $m^3 \cdot ha^{-1}$	269	282	0.39	0.47

the methodology of forest resource assessment and monitoring. Recent studies have demonstrated the advantages of satellite TS in forest inventory, contributing to continuous assessment of forest resources in space and time (Coops et al., 2023; Shang et al., 2020). Unlike many developed countries with more than a century-long history of sample-based forest inventories (Breidenbach et al., 2020), Ukraine has only started to use this approach in 2020. However, the situation in Ukraine is different from other countries that are establishing their forest monitoring programs because of the full-scale Russian invasion. This research provides a basis for integrating various sources of field information with satellite TS to address the need for accurate forest monitoring in the war zone, but also can be used nationally.

In the most forested ecozones, namely the Carpathians and Polissia, the accuracy of our forest mapping approach was the highest. This indicates that forest spatial structure may affect the accuracy of forest maps. For example, forests in the south of Ukraine consist mostly of narrow shelterbelts of 10–15 m width. Thus, individual pixels may simultaneously cover different land cover types and cannot be unambiguously assigned to a single map class. Being more common for coarse spatial resolution data, it causes some problems within highly fragmented forest mosaics even at the 20-m resolution of Sentinel 2 data. The accuracy of the forest map (90–97 %) for ecozones with more than 15 % of forest cover was consistent with similar studies from neighboring countries (Dostálová et al., 2021; Hościło and Lewandowska, 2019). In contrast, forest mapping in the least forested (<10 %) Northern and Southern Steppe ecozones is still challenging. The obtained map accuracies of 59–72 % were significantly lower than in other parts of Ukraine, similar to the performance of forest classification models in mixed forest-pasture landscape mosaics typical for savannas (Mu et al., 2020). The prevalence of omission errors for areas with low percentage of forest cover is well documented in the literature. For example, Zheng et al. (2008) showed that non-prevailing land cover types (i.e., forest in the Steppe ecozones) are likely to be underestimated when the grain size for area estimation is too large compared to forest patch mosaics.

Compared to other studies on tree species mapping, we obtained compatible results (Blickensdörfer et al., 2024; Breidenbach et al., 2021; Hemmerling et al., 2021). Tree species group map accuracies were higher for coniferous species, such as pine and spruce that often grow in pure forest stands. The lowest accuracies were associated with broadleaved tree species. Classification of dominant species in mixed forests faces similar problems as forest mapping in heterogeneous landscapes. Many studies have found that classification accuracy decreases in mixed forest stands (Blickensdörfer et al., 2024) or with increasing pixel size (Hemmerling et al., 2021). Therefore, classification of dominant tree species in the NFI of Ukraine deserves further investigation, particularly with methods that can predict compositional structure at pixel level (Henderson et al., 2014; Van Der Sluijs et al., 2023).

Satellite TS and retrospective forest inventory data support NFI with minimal resources. FMP data played an important role for assessing forests in inaccessible territories affected by the war since 2014. Given the problems posed by territories contaminated by land mines and unexploded ordnance in war-impacted territories, historical field observations including FMP data may be the only available source of information there for a long period of time as plot establishment or stand remeasurement is unlikely.

We also demonstrated that the highly spatially fragmented nature of

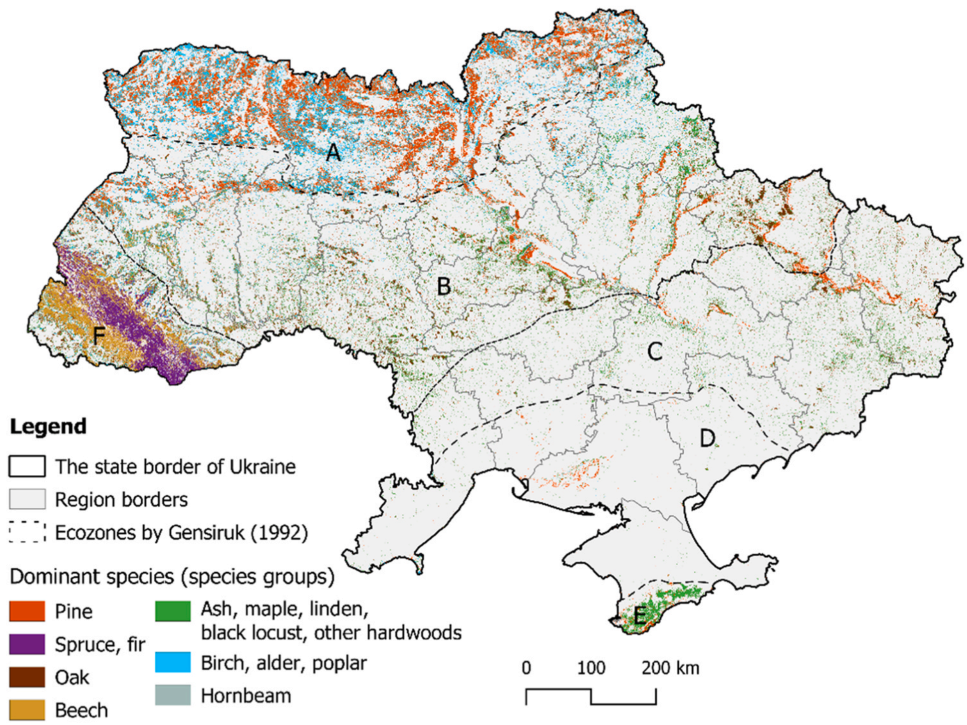

Fig. 5. Dominant species groups in the Ukrainian forests. A – Polissia; B – Forest steppe; C – Northern steppe; D – Southern steppe; E – Crimean Mountains; F – Carpathians.

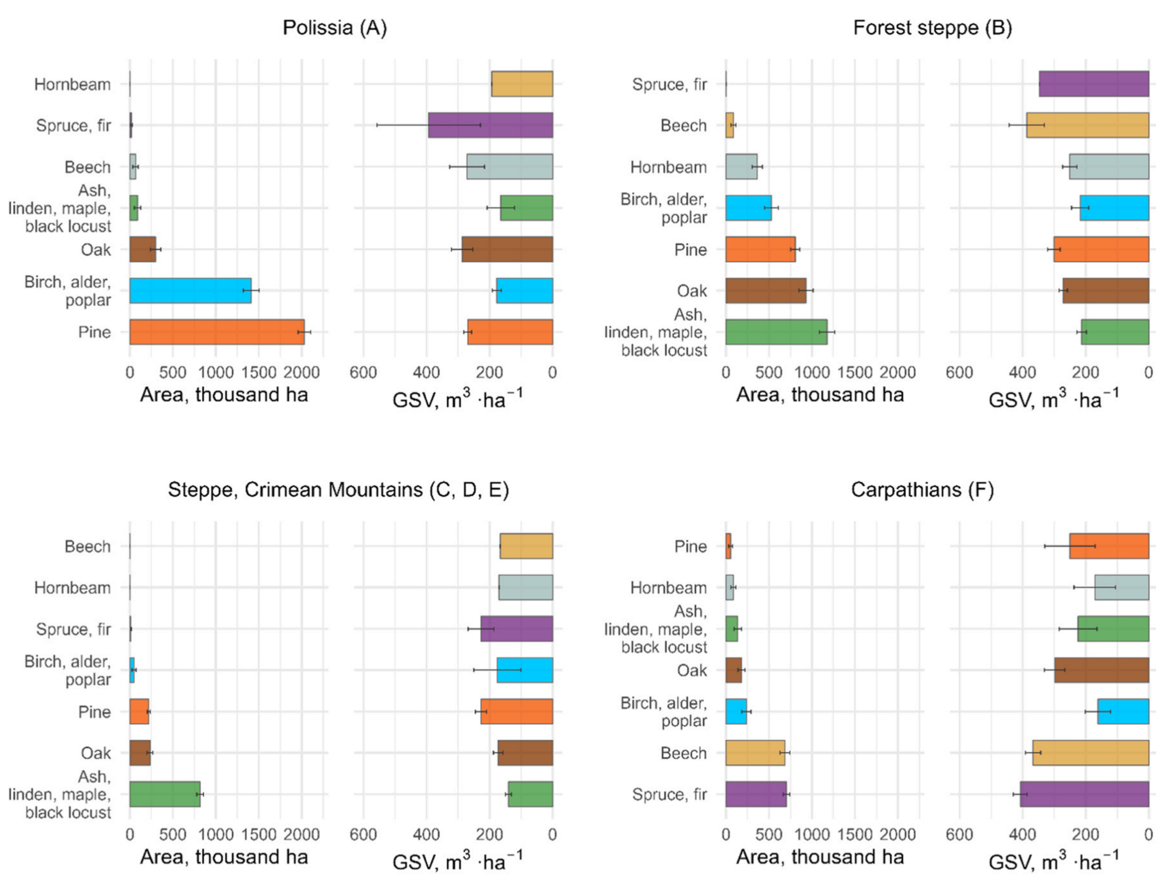

Fig. 6. Forest area and mean GSV of dominant tree species for ecoregions of Ukraine. Error bars indicating the 95 % confidence intervals of the estimates are provided for species with a sufficient number of field observations to apply the GREG estimator.

Table 3
National level assessment of mean values of forest attributes by dominant tree species. Standard errors (SE) of the mean values were obtained using the GREG estimator.

Species (species group)	Age, years		DBH, cm		HT, m		GSV, $m^3 \cdot ha^{-1}$	
	Estimate	SE (%)	Estimate	SE (%)	Estimate	SE (%)	Estimate	SE (%)
All species	57	1.6	28	1.4	20	1.0	251	2.0
All coniferous	58	2.4	29	2.1	21	1.9	299	3.0
All deciduous	57	1.9	27	1.9	19	1.5	226	2.6
Pine	56	2.7	28	2.1	20	2.5	275	3.4
Spruce, fir	63	5.1	31	3.9	22	3.6	406	5.3
Oak	74	3.1	33	3.0	22	2.3	263	3.9
Beech	74	4.6	36	4.2	25	4.0	370	6.1
Ash, linden, maple, black locust	53	4.0	23	4.3	17	2.9	185	5.0
Birch, alder, poplar	43	4.8	24	4.6	19	3.2	185	6.4
Hornbeam	52	6.7	24	7.9	19	6.3	241	8.6

Table 4
Mean values of forest attributes of all forests at ecozone level in Ukraine. Standard errors (SE) of the mean values were obtained using the GREG estimator.

Ecozone	Age, years		DBH, cm		HT, m		GSV, $m^3 \cdot ha^{-1}$	
	Estimate	SE (%)	Estimate	SE (%)	Estimate	SE (%)	Estimate	SE (%)
Polissia	53	2.8	26	2.7	19	2.1	236	3.6
Forest-Steppe	56	2.7	29	2.4	21	1.9	254	3.2
Steppe, Crimean Mountains	62	3.4	23	3.5	16	2.5	163	4.7
Carpathians	62	3.2	31	2.9	22	2.7	331	4.0

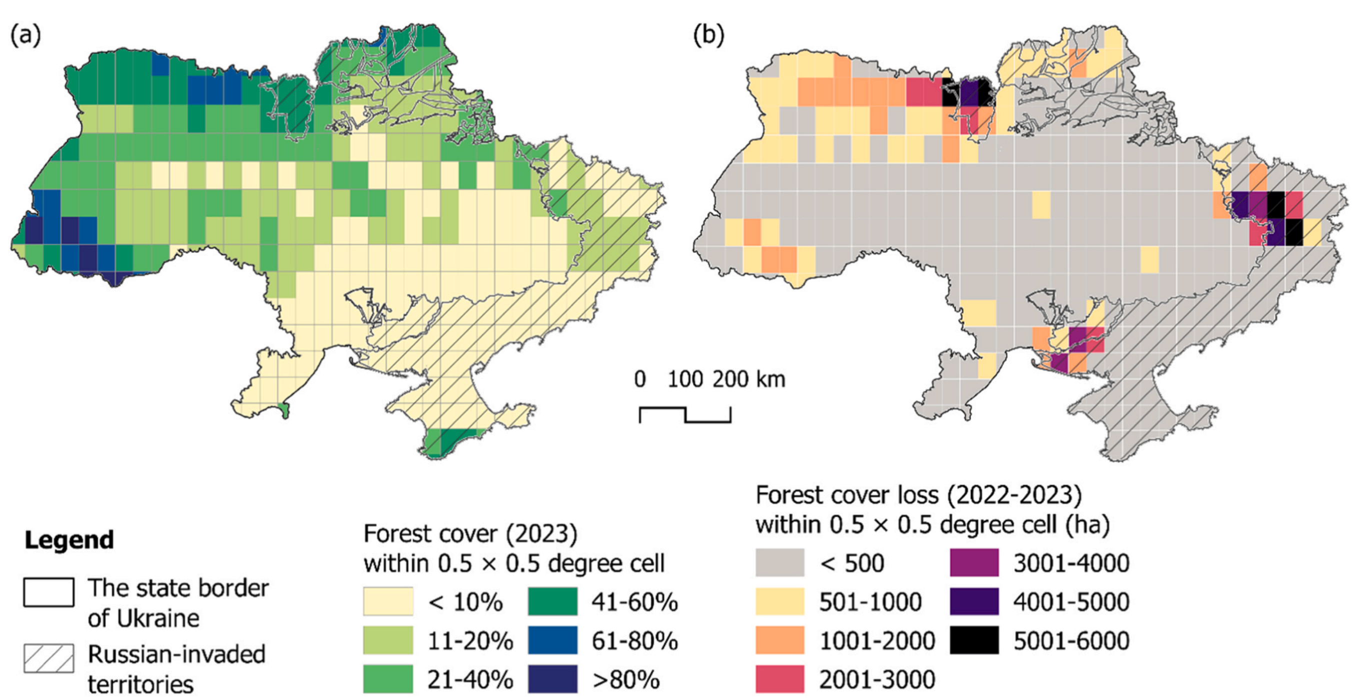

Fig. 7. The spatial pattern of forest cover loss in Ukraine for the period of 2022–2023: (a) represent forest cover aggregated within the regular 0.5 × 0.5 degree grid for 2023; (b) is the total forest area loss between 2022 and 2023 extracted within the corresponding grid using Sentinel 2 TS.

Ukrainian forests poses significant problems for NFI (Fig. 9). In particular, the current regulations limit the size of clear-cuts to 3–5 ha, resulting in very patchy mosaics of forested and temporarily unforested areas. In this situation, the accurate determination of plot center coordinates is critical to obtain a good spatial link between forest characteristics and pixel data. Furthermore, many NFI plots may be close to forest edges, leading to spectrally mixed pixels and degrading the quality of predictive models. As a result, the values of the coefficient of determination were higher for the GNN model developed using the FMP data ($R^2 = 0.62$) than for those using the NFI data ($R^2 = 0.41$). Although this situation leads us to consider more carefully the quality of the NFI data collected in highly fragmented forests throughout Ukraine, we did not find any negative impact of the combined use of FMP and NFI data for nationwide forest resource assessment, including inaccessible areas.

Our study has shown that scale should be taken into account when reporting the NFI. The nationwide estimates based on a complete dataset of reference observations were calculated with the lowest standard errors. We also obtained estimates of forest attributes at the ecozone level for which we had enough field observations. Although we do not calculate standard errors at the spatial scale of oblasts, the results can be

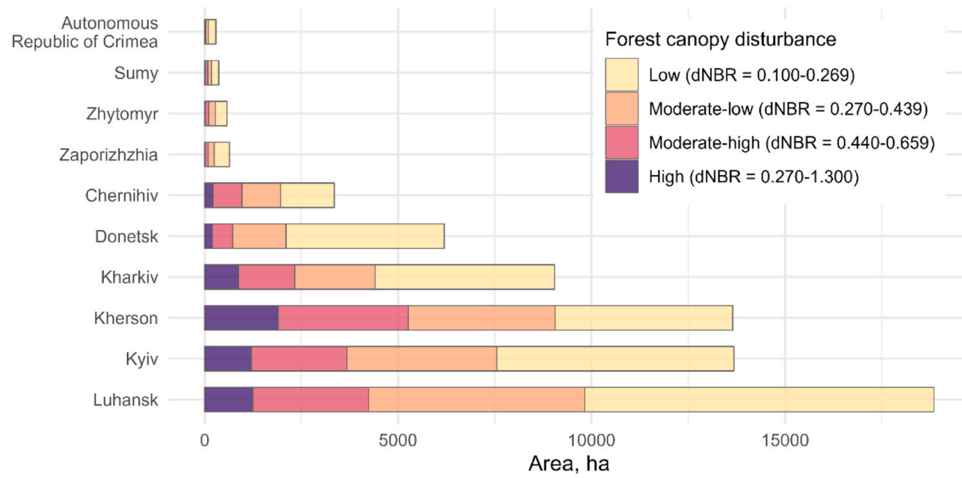

Fig. 8. Distribution of the forest area by levels of canopy disturbance within the war-affected areas.

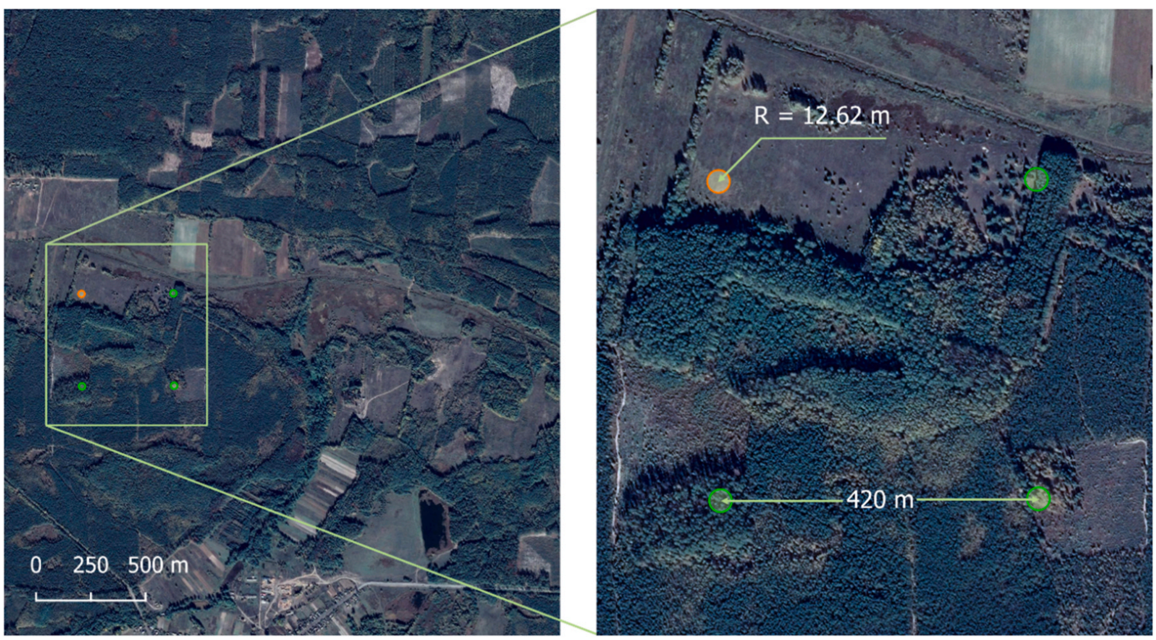

Fig. 9. An example of potential problem with accuracy of mapped attributes in highly fragmented forests of Ukraine. Green circles represent forested NFI plots located either on or near forest edges, orange circle is an unforested plot.

obtained from 20-m spatial resolution maps. These maps are important assets of the remote sensing-based NFI providing valuable insights into the forest characteristics over Ukraine. At stand- and landscape-levels, where few if any NFI plots may be available, those maps offer an opportunity to generate model-based forest attribute estimation in support of planning (Bell et al., 2022, p. 202; McRoberts, 2012).

The CCDC temporal segmentation algorithm was a particularly useful element of our mapping workflow, allowing historical field observations to be linked to spectral data. This is a great methodological advance over other studies that use temporal image mosaics (Breidenbach et al., 2021). Continuous monitoring of forest cover change using the CCDC-based approach has been successfully demonstrated in many recent studies (Brown et al., 2020; Chen, 2021; Myroniuk et al., 2022). However, its utility for temporally consistent investigations of forest attribute change at the pixel level has not been adequately addressed. Given the results obtained by Wilson et al. (2018), there are great prospects for the application of temporally smoothed Sentinel 2 TS to track structural changes in forests (biomass, GSV, DBH, etc.). In addition, the incorporation of adjusted SAR Sentinel 1 data (Bullock et al., 2022) seems to be a very promising option to further advance our mapping approach.

4.2. *Potential for spatial assessment of war-induced forest damage*

Quantifying war-damaged forests in Ukraine is an urgent task of high importance. Damage information is requested by Ukrainian government organizations to assess the monetary value of war-related losses as well as by international organizations and NGOs. Reconstruction and rehabilitation needs consider different types of environmental impacts. Therefore, many recent studies have incorporated remote sensing to provide quantitative assessments of war impacts on agriculture (Kussul et al., 2023), protected areas (Shumilo et al., 2023), forests (Irland et al., 2023; Matsala et al., 2024), and greenhouse gas emissions (Bun et al., 2024). It is likely that many new studies on this topic will be published in the near future. However, such efforts may be fragmented and lead to conflicting results for forest damage assessment due to inconsistent methodologies. Here, we presented a nationwide baseline for comprehensive accounting of war-induced forest damage using existing reliable forest inventory and remote sensing data.

The current work has a wide range of implications for war damage assessment. In particular, we have estimated that approximately 1.7 million hectares of forest (15 % of the entire forested area in Ukraine) could be potentially affected by the war. This information is crucial for the delineation of mined forested areas and the coordination of landmine clearance efforts in Ukraine. Importantly, forested areas in proximity to the national border, active frontline or line of contact without detected canopy damage (as sign of battles and shelling) may indirectly indicate the abundant installation of landmines. In this regard, comprehensive products based on satellite TS will help to guide long-term impacts of war, as on the Korean Peninsula (Dong et al., 2020). In addition to this broader geography of forests potentially affected by the war, 67,000 ha of forest were disturbed within that war footprint during the war. Additional information and analysis are needed in order to reliably attribute such damage to causal agents related to the war, such as fire or illegal timber harvesting. Furthermore, there is a need to understand both immediate damages, such as damaged timber, and long-term forest recovery.

An important aspect of future work is the estimation of species and biomass losses relevant to different levels of forest cover change. A challenging prospect will be to connect spectral recovery to 'true' (functional) forest restoration using satellite TS (Gorsevski et al., 2012). Hopefully, this study will provide a valuable framework to address all these data needs and to provide national reporting on forest resources in war-affected Ukraine.

5. Conclusions

This paper presents the motivations, needs, methodology, and results of the first remote sensing-based inventory in Ukraine. The developed approach provides a framework for nationwide estimation of forest resources in a situation where large areas remain inaccessible or not controlled by the government. We have demonstrated that Sentinel 2 TS combined with retrospective field observations can provide up-to-date information on forest resources. This is an important feature of the developed methodology as the war in Ukraine is ongoing and there is a constant need for timely information on forests. The advantages of remote sensing in the Ukrainian NFI are also that it can now provide spatially explicit information with statistical estimates. As new field observations become available, the results can be better structured at lower spatial scales (i.e. administrative oblasts, protected areas, hromadas, etc.). Currently, the temporally smoothed Sentinel 2 TS and the developed output maps can be integrated into large-scale forest change analyses over Ukraine, including war-affected areas.

CRediT authorship contribution statement

Viktor Myroniuk: Writing – review & editing, Writing – original draft, Visualization, Validation, Software, Methodology, Formal analysis, Data curation, Conceptualization. **Axel Weinreich:** Methodology, Conceptualization. **Vincent von Dosky:** Visualization, Data curation. **Viktor Melnychenko:** Resources. **Andrii Shamrai:** Validation, Resources. **Maksym Matsala:** Writing – review & editing, Writing – original draft, Formal analysis. **Matthew J. Gregory:** Writing – review & editing, Writing – original draft, Software. **David M. Bell:** Writing – review & editing, Writing – original draft. **Raymond Davis:** Writing – review & editing, Writing – original draft.

Declaration of Competing Interest

The authors declare that they have no known competing financial interests or personal relationships that could have appeared to influence the work reported in this paper.

Data availability

Data will be made available on request.

Acknowledgements

This research was conducted with the support of the project W-UKR 21–01 "Technical Support to Forest Policy Development and National Forest Inventory Implementation" (SFI), which was established within the framework of the Bilateral Cooperation Program (BCP) of the Federal Ministry of Food and Agriculture of Germany (BMEL). The authors would like to thank Dr. Heino Polley and Dr. Matthias Dees for their contributions to the formal analysis of the study results.

References

Bell, D.M., Acker, S.A., Gregory, M.J., Davis, R.J., Garcia, B.A., 2021. Quantifying regional trends in large live tree and snag availability in support of forest management. For. Ecol. Manag. *479*, 118554 https://doi.org/10.1016/j.foreco.2020.118554.

Bell, D.M., Wilson, B.T., Werstak, C.E., Oswalt, C.M., Perry, C.H., 2022. Examining k-nearest neighbor small area estimation across scales using national forest inventory data. Front. For. Glob. Change *5*, 763422. https://doi.org/10.3389/ffgc.2022.763422.

Bey, A., Sánchez-Paus Díaz, A., Maniatis, D., Marchi, G., Mollicone, D., Ricci, S., Bastin, J.-F., Moore, R., Federici, S., Rezende, M., Patriarca, C., Turia, R., Gamoga, G., Abe, H., Kaidong, E., Miceli, G., 2016. Collect earth: land use and land cover assessment through augmented visual interpretation. Remote Sens. *8* (10), 807. https://doi.org/10.3390/rs8100807.

Bilous, A.M., Kashpor, S.M., Myroniuk, V.V., Svynchyk, V.A., Lesnik, O.M., 2020. in Ukrainian. In: Forest Inventory Handbook, 2020. Lira LTD, Dnipro, p. 364.

Blickensdörfer, L., Oehmichen, K., Pflugmacher, D., Kleinschmit, B., Hostert, P., 2024. National tree species mapping using Sentinel-1/2 time series and German National Forest Inventory data. Remote Sens. Environ. *304*, 114069 https://doi.org/10.1016/j.rse.2024.114069.

Bravo-Oviedo, A., Pretzsch, H., Ammer, C., Andenmatten, E., Barbati, A., Barreiro, S., Brang, P., Bravo, F., Coll, L., Corona, P., Den Ouden, J., Ducey, M.J., Forrester, D.I., Giergiczny, M., Jacobsen, J.B., Lesinski, J., Löf, M., Mason, W.L., Matovic, B., Zlatanov, T., 2014. European mixed forests: definition and research perspectives. For. Syst. *23* (3), 518–533. https://doi.org/10.5424/fs/2014233-06256.

Breidenbach, J., Granhus, A., Hylen, G., Eriksen, R., Astrup, R., 2020. A century of National Forest Inventory in Norway – informing past, present, and future decisions. For. Ecosyst. *7* (1), 46. https://doi.org/10.1186/s40663-020-00261-0.

Breidenbach, J., Waser, L.T., Debella-Gilo, M., Schumacher, J., Rahlf, J., Hauglin, M., Puliti, S., Astrup, R., 2021. National mapping and estimation of forest area by dominant tree species using Sentinel-2 data. Can. J. For. Res. *51* (3), 365–379. https://doi.org/10.1139/cjfr-2020-0170.

Breiman, L., 2001. Random forests. Mach. Learn. *45* (1), 5–32. https://doi.org/10.1023/a:1010933404324.

Brosofske, K.D., Froese, R.E., Falkowski, M.J., Banskota, A., 2014. A review of methods for mapping and prediction of inventory attributes for operational forest management. For. Sci. *60* (4), 733–756. https://doi.org/10.5849/forsci.12-134.

Brown, J.F., Tollerud, H.J., Barber, C.P., Zhou, Q., Dwyer, J.L., Vogelmann, J.E., Loveland, T.R., Woodcock, C.E., Stehman, S.V., Zhu, Z., Pengra, B.W., Smith, K., Horton, J.A., Xian, G., Auch, R.F., Sohl, T.L., Sayler, K.L., Gallant, A.L., Zelenak, D., Rover, J., 2020. Lessons learned implementing an operational continuous United States national land change monitoring capability: the land change monitoring, assessment, and projection (LCMAP) approach. Remote Sens. Environ. *238*, 111356 https://doi.org/10.1016/j.rse.2019.111356.

Bullock, E.L., Healey, S.P., Yang, Z., Houborg, R., Gorelick, N., Tang, X., Andrianirina, C., 2022. Timeliness in forest change monitoring: a new assessment framework demonstrated using Sentinel-1 and a continuous change detection algorithm. Remote Sens. Environ. *276*, 113043 https://doi.org/10.1016/j.rse.2022.113043.

Bun, R., Marland, G., Oda, T., See, L., Puliafito, E., Nahorski, Z., Jonas, M., Kovalyshyn, V., Ialongo, I., Yashchun, O., Romanchuk, Z., 2024. Tracking unaccounted greenhouse gas emissions due to the war in Ukraine since 2022. Sci. Total Environ. *914*, 169879 https://doi.org/10.1016/j.scitotenv.2024.169879.

Chen, S., 2021. Monitoring temperate forest degradation on Google Earth Engine using Landsat time series analysis. Remote Sens. Environ. 22.

Chirici, G., Giannetti, F., McRoberts, R.E., Travaglini, D., Pecchi, M., Maselli, F., Chiesi, M., Corona, P., 2020. Wall-to-wall spatial prediction of growing stock volume based on Italian National Forest Inventory plots and remotely sensed data. Int. J. Appl. Earth Obs. Geoinf. *84*, 101959 https://doi.org/10.1016/j.jag.2019.101959.

Chirici, G., Mura, M., McInerney, D., Py, N., Tomppo, E.O., Waser, L.T., Travaglini, D., McRoberts, R.E., 2016. A meta-analysis and review of the literature on the k-Nearest Neighbors technique for forestry applications that use remotely sensed data. Remote Sens. Environ. *176*, 282–294. https://doi.org/10.1016/j.rse.2016.02.001.

Coops, N.C., Tompalski, P., Goodbody, T.R.H., Achim, A., Mulverhill, C., 2023. Framework for near real-time forest inventory using multi source remote sensing data. For.: Int. J. For. Res. *96* (1), 1–19. https://doi.org/10.1093/forestry/cpac015.

Davis, R.J., Bell, D.M., Gregory, M.J., Yang, Z., Gray, A.N., Healey, S.P., & Stratton, A.E. (2022). *Northwest Forest Plan—the first 25 years (1994–2018): Status and trends of late-successional and old-growth forests* (Gen. Tech. Rep. PNW-GTR-1004; p. 82). U.S. Department of Agriculture, Forest Service, Pacific Northwest Research Station. https://doi.org/10.2737/PNW-GTR-1004.

Dong, Y., Ren, Z., Wang, Z., Yu, Q., Zhu, L., Yu, H., Bao, G., 2020. Spatiotemporal patterns of forest changes in korean peninsula using landsat images during 1990–2015: a comparative study of two neighboring countries. IEEE Access *8*, 73623–73633. https://doi.org/10.1109/ACCESS.2020.2988122.

Dostálová, A., Lang, M., Ivanovs, J., Waser, L.T., Wagner, W., 2021. European wide forest classification based on sentinel-1 data. Remote Sens. *13* (3), 337. https://doi.org/10.3390/rs13030337.

Fassnacht, F.E., Latifi, H., Stereńczak, K., Modzelewska, A., Lefsky, M., Waser, L.T., Straub, C., Ghosh, A., 2016. Review of studies on tree species classification from remotely sensed data. Remote Sens. Environ. *186*, 64–87. https://doi.org/10.1016/j.rse.2016.08.013.

Fassnacht, F.E., White, J.C., Wulder, M.A., Næsset, E., 2024. Remote sensing in forestry: current challenges, considerations and directions. For.: Int. J. For. Res. *97* (1), 11–37. https://doi.org/10.1093/forestry/cpad024.

Gensiruk, S.A. (1992). *Forests of Ukraine*. Kyiv: Naukova dumka (in Ukrainian).

Gorelick, N., Hancher, M., Dixon, M., Ilyushchenko, S., Thau, D., Moore, R., 2017. Google earth engine: planetary-scale geospatial analysis for everyone. Remote Sens. Environ. *202*, 18–27. https://doi.org/10.1016/j.rse.2017.06.031.

Gorelick, N., Yang, Z., Arévalo, P., Bullock, E.L., Insfrán, K.P., Healey, S.P., 2023. A global time series dataset to facilitate forest greenhouse gas reporting. Environ. Res. Lett. *18* (8), 084001 https://doi.org/10.1088/1748-9326/ace2da.

Gorsevski, V., Kasischke, E., Dempewolf, J., Loboda, T., Grossmann, F., 2012. Analysis of the impacts of armed conflict on the eastern afromontane forest region on the South Sudan—Uganda border using multitemporal Landsat imagery. Remote Sens. Environ. *118*, 10–20. https://doi.org/10.1016/j.rse.2011.10.023.

2012 Handbook of the Forest Fund of Ukraine based on the State Forest Assessment as of 01.01.2011. (2012). State Forest Inventory Enterprise.

Hemmerling, J., Pflugmacher, D., Hostert, P., 2021. Mapping temperate forest tree species using dense Sentinel-2 time series. Remote Sens. Environ. *267*, 112743 https://doi.org/10.1016/j.rse.2021.112743.

Henderson, E.B., Bell, D.M., Gregory, M.J., 2019. Vegetation mapping to support greater sage-grouse habitat monitoring and management: multi- or univariate approach? Ecosphere *10* (8). https://doi.org/10.1002/ecs2.2838.

Henderson, E.B., Ohmann, J.L., Gregory, M.J., Roberts, H.M., Zald, H., 2014. Species distribution modelling for plant communities: stacked single species or multivariate modelling approaches? Appl. Veg. Sci. *17* (3), 516–527. https://doi.org/10.1111/avsc.12085.

Hermosilla, T., Wulder, M.A., White, J.C., Coops, N.C., 2022. Land cover classification in an era of big and open data: optimizing localized implementation and training data selection to improve mapping outcomes. Remote Sens. Environ. *268*, 112780 https://doi.org/10.1016/j.rse.2021.112780.

Hislop, S., Haywood, A., Alaibakhsh, M., Nguyen, T.H., Soto-Berelov, M., Jones, S., Stone, C., 2021. A reference data framework for the application of satellite time series to monitor forest disturbance. Int. J. Appl. Earth Obs. Geoinf. *105*, 102636 https://doi.org/10.1016/j.jag.2021.102636.

Hościło, A., Lewandowska, A., 2019. Mapping forest type and tree species on a regional scale using multi-temporal sentinel-2 data. Remote Sens. *11* (8), 929. https://doi.org/10.3390/rs11080929.

Irland, L.C., Iavorivska, L., Zibtsev, S., Myroniuk, V., Roth, B., Bilous, A., 2023. Russian invasion: rapid assessment of impact on Ukraine's forests. Procidings For. Acad. Sci. Ukr. *25*, 146–155. https://doi.org/10.15421/412312.

James, G., Witten, D., Hastie, T., & Tibshirani, R. (Eds.). (2013). An introduction to statistical learning: With applications in R. Springer.

Kennedy, R.E., Ohmann, J., Gregory, M., Roberts, H., Yang, Z., Bell, D.M., Kane, V., Hughes, M.J., Cohen, W.B., Powell, S., Neeti, N., Larrue, T., Hooper, S., Kane, J., Miller, D.L., Perkins, J., Braaten, J., Seidl, R., 2018. An empirical, integrated forest biomass monitoring system. Environ. Res. Lett. *13* (2), 025004 https://doi.org/10.1088/1748-9326/aa9d9e.

Kennedy, R.E., Yang, Z., Cohen, W.B., 2010. Detecting trends in forest disturbance and recovery using yearly Landsat time series: 1. LandTrendr – Temporal segmentation algorithms. Remote Sens. Environ. *114* (12), 2897–2910. https://doi.org/10.1016/j.rse.2010.07.008.

Kershaw, J.A., Ducey, M.J., Beers, T., & Hush, B. (2016). *Forest Mensuration, 5th ed.*

Key, C.H., & Benson, N.C. (2006). Landscape Assessment (LA): Sampling and Analysis Methods (General Technical Report RMRS-GTR-164; FIREMON: Fire Effects Monitoring and Inventory System, p. LA-1-LA-51). Rocky Mountain Research Station, US Department of Agriculture, Forest Service.

Kussul, N., Drozd, S., Yailymova, H., Shelestov, A., Lemoine, G., Deininger, K., 2023. Assessing damage to agricultural fields from military actions in Ukraine: an integrated approach using statistical indicators and machine learning. Int. J. Appl. Earth Obs. Geoinf. *125*, 103562 https://doi.org/10.1016/j.jag.2023.103562.

Lister, A.J., Andersen, H., Frescino, T., Gatziolis, D., Healey, S., Heath, L.S., Liknes, G.C., McRoberts, R., Moisen, G.G., Nelson, M., Riemann, R., Schleeweis, K., Schroeder, T. A., Westfall, J., Wilson, B.T., 2020. Use of remote sensing data to improve the efficiency of national forest inventories: a case study from the united states national forest inventory. Forests *11* (12), 1364. https://doi.org/10.3390/f11121364.

Maltman, J.C., Hermosilla, T., Wulder, M.A., Coops, N.C., White, J.C., 2023. Estimating and mapping forest age across Canada's forested ecosystems. Remote Sens. Environ. *290*, 113529 https://doi.org/10.1016/j.rse.2023.113529.

Matasci, G., Hermosilla, T., Wulder, M.A., White, J.C., Coops, N.C., Hobart, G.W., Zald, H.S.J., 2018. Large-area mapping of Canadian boreal forest cover, height, biomass and other structural attributes using Landsat composites and lidar plots. Remote Sens. Environ. *209*, 90–106. https://doi.org/10.1016/j.rse.2017.12.020.

Matsala, M., Bilous, A., Myroniuk, V., Holiaka, D., Schepaschenko, D., See, L., Kraxner, F., 2021. The return of nature to the chernobyl exclusion zone: increases in forest cover of 1.5 times since the 1986 disaster. Forests *12* (8), 1024. https://doi.org/10.3390/f12081024.

Matsala, M., Odruzhenko, A., Hinchuk, T., Myroniuk, V., Drobyshev, I., Sydorenko, S., Zibtsev, S., Milakovsky, B., Schepaschenko, D., Kraxner, F., Bilous, A., 2024. War drives forest fire risks and highlights the need for more ecologically-sound forest management in post-war Ukraine. Sci. Rep. *14* (1), 4131. https://doi.org/10.1038/s41598-024-54811-5.

McConville, K.S., Moisen, G.G., Frescino, T.S., 2020. A tutorial on model-assisted estimation with application to forest inventory. Forests *11* (2), 244. https://doi.org/10.3390/f11020244.

McRoberts, R.E., 2012. Estimating forest attribute parameters for small areas using nearest neighbors techniques. For. Ecol. Manag. *272*, 3–12. https://doi.org/10.1016/j.foreco.2011.06.039.

McRoberts, R.E., Næsset, E., Gobakken, T., 2014. Estimation for inaccessible and non-sampled forest areas using model-based inference and remotely sensed auxiliary information. Remote Sens. Environ. *154*, 226–233. https://doi.org/10.1016/j.rse.2014.08.028.

McRoberts, R.E., Tomppo, E., 2007. Remote sensing support for national forest inventories. Remote Sens. Environ. *110* (4), 412–419. https://doi.org/10.1016/j.rse.2006.09.034.

Mu, Y., Biggs, T., Stow, D., Numata, I., 2020. Mapping heterogeneous forest-pasture mosaics in the Brazilian Amazon using a spectral vegetation variability index, band transformations and random forest classification. Int. J. Remote Sens. *41* (22), 8682–8692. https://doi.org/10.1080/2150704X.2020.1802529.

Myroniuk, V., Bell, D.M., Gregory, M.J., Vasylyshyn, R., Bilous, A., 2022. Uncovering forest dynamics using historical forest inventory data and Landsat time series. For. Ecol. Manag. *513*, 120184 https://doi.org/10.1016/j.foreco.2022.120184.

Ohmann, J.L., Gregory, M.J., Roberts, H.M., Cohen, W.B., Kennedy, R.E., Yang, Z., 2012. Mapping change of older forest with nearest-neighbor imputation and Landsat time-series. For. Ecol. Manag. *272*, 13–25. https://doi.org/10.1016/j.foreco.2011.09.021.

Ohmann, J.L., Gregory, M.J., 2002. Predictive mapping of forest composition and structure with direct gradient analysis and nearest- neighbor imputation in coastal Oregon, U.S.A. Can. J. For. Res. *32* (4), 725–741. https://doi.org/10.1139/x02-011.

Olofsson, P., Foody, G.M., Herold, M., Stehman, S.V., Woodcock, C.E., Wulder, M.A., 2014. Good practices for estimating area and assessing accuracy of land change. Remote Sens. Environ. *148*, 42–57. https://doi.org/10.1016/j.rse.2014.02.015.

Pasquarella, V.J., Arévalo, P., Bratley, K.H., Bullock, E.L., Gorelick, N., Yang, Z., Kennedy, R.E., 2022. Demystifying landtrendr and CCDC temporal segmentation. Int. J. Appl. Earth Obs. Geoinf. *110*, 102806 https://doi.org/10.1016/j.jag.2022.102806.

Riley, K.L., Grenfell, I.C., Finney, M.A., 2016. Mapping forest vegetation for the western United States using modified random forests imputation of FIA forest plots. Ecosphere *7* (10), e01472. https://doi.org/10.1002/ecs2.1472.

Senf, C., Seidl, R., 2021. Mapping the forest disturbance regimes of Europe. Nat. Sustain. *4* (1), 63–70. https://doi.org/10.1038/s41893-020-00609-y.

Shang, C., Coops, N.C., Wulder, M.A., White, J.C., Hermosilla, T., 2020. Update and spatial extension of strategic forest inventories using time series remote sensing and modeling. Int. J. Appl. Earth Obs. Geoinf. *84*, 101956 https://doi.org/10.1016/j.jag.2019.101956.

Shumilo, L., Skakun, S., Gore, M.L., Shelestov, A., Kussul, N., Hurtt, G., Karabchuk, D., Yarotskiy, V., 2023. Conservation policies and management in the Ukrainian Emerald Network have maintained reforestation rate despite the war. Commun. Earth Environ. *4* (1), 443. https://doi.org/10.1038/s43247-023-01099-4.

Stefanski, J., Chaskovskyy, O., Waske, B., 2014. Mapping and monitoring of land use changes in post-Soviet western Ukraine using remote sensing data. Appl. Geogr. *55*, 155–164. https://doi.org/10.1016/j.apgeog.2014.08.003.

Storozhuk, V., & Polley, H. (2017). Forest Inventory—Status Quo in Ukraine, Experience of Germany, and FAO Recommendations (Agricultural Policy Report APD/APB/06/2017; p. 52). German-Ukrainian Agricultural Policy Dialogue. https://www.apd-ukraine.de/images/2018/APR/APD_APR_07-2017_Forest_Inventories_ukr.pdf (in Ukrainian).

Van Der Sluijs, J., Peddle, D.R., Hall, R.J., 2023. Characterizing tree species in northern boreal forests using multiple-endmember spectral mixture analysis and multi-temporal satellite imagery. Can. J. Remote Sens. *49* (1), 2216312 https://doi.org/10.1080/07038992.2023.2216312.

Welle, T., Aschenbrenner, L., Kuonath, K., Kirmaier, S., Franke, J., 2022. Mapping dominant tree species of German forests. Remote Sens. *14* (14), 3330. https://doi.org/10.3390/rs14143330.

Wilson, B.T., Knight, J.F., McRoberts, R.E., 2018. Harmonic regression of Landsat time series for modeling attributes from national forest inventory data. ISPRS J. Photogramm. Remote Sens. *137*, 29–46. https://doi.org/10.1016/j.isprsjprs.2018.01.006.

Xian, G.Z., Smith, K., Wellington, D., Horton, J., Zhou, Q., Li, C., Auch, R., Brown, J.F., Zhu, Z., Reker, R.R., 2022. Implementation of the CCDC algorithm to produce the LCMAP collection 1.0 annual land surface change product. Earth Syst. Sci. Data *14* (1), 143–162. https://doi.org/10.5194/essd-14-143-2022.

Zheng, D., Heath, L.S., Ducey, M.J., 2008. Identifying grain-size dependent errors on global forest area estimates and carbon studies. Geophys. Res. Lett. *35* (21), 2008GL035746 https://doi.org/10.1029/2008GL035746.

Zhu, Z., 2017. Change detection using landsat time series: a review of frequencies, preprocessing, algorithms, and applications. ISPRS J. Photogramm. Remote Sens. *130*, 370–384. https://doi.org/10.1016/j.isprsjprs.2017.06.013.

Zhu, Z., Woodcock, C.E., 2014. Continuous change detection and classification of land cover using all available Landsat data. Remote Sens. Environ. *144*, 152–171. https://doi.org/10.1016/j.rse.2014.01.011.